Realizing quantum spin liquid phases in spin-orbit driven correlated materials

Andrei Catuneanu,[1] Youhei Yamaji,[2,3] Gideon Wachtel,[1] Hae-Young Kee,[1,4] and Yong Baek Kim[1,4]

[1] *Department of Physics and Center for Quantum Materials, University of Toronto, 60 St. George St., Toronto, Ontario, M5S 1A7, Canada*
[2] *Department of Applied Physics and Quantum-Phase Electronics Center (QPEC), The University of Tokyo, Hongo, Bunkyo-ku, Tokyo, 113-8656, Japan*
[3] *JST, PRESTO, Hongo, Bunkyo-ku, Tokyo, 113-8656, Japan*
[4] *Canadian Institute for Advanced Research, Toronto, Ontario, M5G 1Z8, Canada*

The spin liquid phase is one of the prominent strongly interacting topological phases of matter whose unambiguous confirmation is yet to be reached despite intensive experimental efforts on numerous candidate materials. The challenge is derived from the difficulty of formulating realistic theoretical models for these materials and interpreting the corresponding experimental data. Here we study a theoretical model with bond-dependent interactions, directly motivated by recent experiments on two-dimensional correlated materials with strong spin-orbit coupling. We show numerical evidence for the existence of an extended family of quantum spin liquids, which are possibly connected to the Kitaev spin liquid state. These results are used to provide an explanation of the scattering continuum seen in neutron scattering on α-$RuCl_3$. Implications of these results to three-dimensional materials such as hyperhoneycomb iridate, β-Li_2IrO_3, are also discussed.

arXiv:1701.07837v1 [cond-mat.str-el] 26 Jan 2017

Introduction — The role of strong interaction between electrons in the emergence of topological phases of matter, where both theoretical and experimental understanding is far from complete compared to weakly interacting systems, has recently been a topic of intensive research. The archetypal example of a topological phase with strong electron interaction is the quantum spin liquid[1], in which the elementary excitations are charge-neutral fractionalized particles. While a lot of progress has been made on the theoretical understanding of the quantum spin liquid phase, its direct experimental confirmation has remained elusive despite various studies on a number of candidate materials[2–6]. Significant progress, however, has recently been made due to the availabilty of a new class of correlated materials, where strong spin-orbit coupling leads to various bond-dependent spin interactions[7–9]. These materials are Mott insulators with $4d$ and $5d$ transition metal elements, which include iridates and ruthenates with two-dimensional honeycomb lattice[10,11] and three-dimensional variants[12,13].

Magnetic frustration in these new systems arises from bond-dependent interactions[7,14–18] rather than relying on the geometric frustration of the underlying lattice structure used in earlier approaches. These materials are of great interest because they may intrinsically generate the Kitaev interaction which, in the absence of other interactions, would lead to a material realization of an exactly solvable model for the quantum spin liquid phase[19]. This raises the question for the stability of the Kitaev spin liquid against other perturbations always present in a real material. In some known models, the Kitaev spin liquid phase is stable only for sufficiently small magnitudes of other interactions[14,20–24], making its experimental realization a challenging endeavor.

In this work, we analyze a theoretical model that may host an extended family of quantum spin liquid phases and make connections to recent experiments on a number of 4d and 5d transition metal oxide materials. We consider the following nearest-neighbor (n.n.) model on a two-dimensional honeycomb lattice:

$$H = \sum_{\gamma \in x,y,z} H^{\gamma}, \tag{1}$$

where

$$H^{z} = \sum_{\langle ij \rangle \in z-bond} [K_z S_i^z S_j^z + \Gamma_z (S_i^x S_j^y + S_i^y S_j^x)] \tag{2}$$

and $H^{x,y}$ are defined similarly with corresponding $K_{x,y}$ and $\Gamma_{x,y}$. Each H^{γ} represents the n.n spin interactions along one of the three bond directions, $\gamma = x, y, z$. The model is parameterized by $K_z = -(1+2a)\cos\phi$, $K_{x,y} = -(1-a)\cos\phi$, $\Gamma_{x,y,z} = \sin\phi$, with a characterizing bond anisotropy. When $\phi = 0, \pi$ (i.e. $\Gamma_\gamma = 0$), this model reduces to the exactly solvable Kitaev model with a quantum spin liquid ground state. Moreover, a recent analysis in the $\phi = \pi/2$ limit (i.e. $K_\gamma = 0$) revealed a macroscopically degenerate ground state in the classical model[25].

The above model is directly motivated by experiments on α-$RuCl_3$ ($RuCl_3$) and earlier *ab initio* computations. In $RuCl_3$, Ru^{3+} ions carry a spin-orbit entangled pseudospin-1/2 degree of freedom and sit on a two-dimensional honeycomb lattice. *Ab initio* computations suggest that the dominant spin exchange interactions are given by $K_\gamma < 0$ and $\Gamma_\gamma > 0$ with comparable magnitude as well as a non-negligible 3rd n.n. antiferromagnetic Heisenberg interaction $J_3 > 0$[26–29]. In addition, it was found that both K_γ and Γ_γ are slightly anisotropic and that J_3 may promote the zig-zag magnetic order observed experimentally[27,28]. On the other hand, a recent inelastic neutron scattering experiment observed finite energy scattering continua reminiscent of the excitation spectra in quantum spin liquid phases, both above and below the magnetic ordering transition temperature, potentially indicating proximity to a quantum spin liquid phase[30]. While this interpretation is natural, it is not obvious what kind of quantum spin liquid may be nearby given that the relevant microscopic model is far from the ideal Kitaev limit.

Here we take the Hamiltonian in Eq. (1) as the minimal model for the putative quantum spin liquid phase and

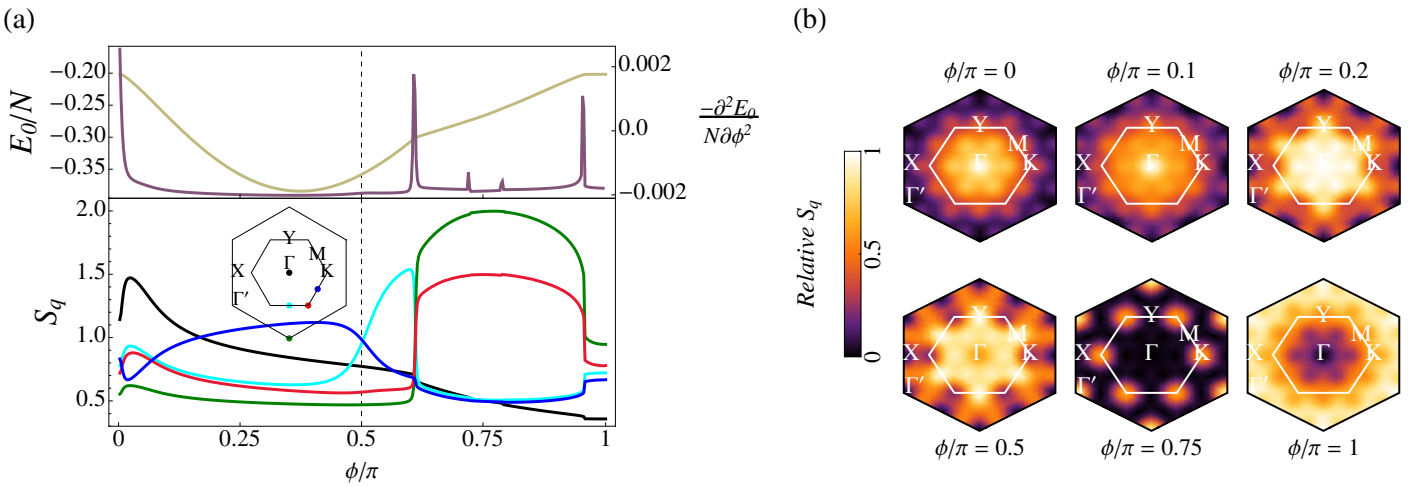

FIG. 1. (Color online) (a) *Top:* E_0/N (yellow) and $-\frac{1}{N}\frac{\partial^2 E_0}{\partial\phi^2}$ (purple) for anisotropy parameter $a = 0.1$. *Bottom:* S_q for anisotropy parameter $a = 0.1$ at Γ- (black), M- (blue), Y- (cyan), K- (red) and Γ′- (green) in the reciprocal lattice (inset). (b) Representation of S_q, averaged over domains in a real material, when $a = 0.1$ for various ϕ in the phase diagram.

treat J_3 as a perturbation. We study this model using three different numerical methods which combined together give the following results:
1) When K_γ has the ferromagnetic sign ($0 \le \phi \le \pi/2$), there is no phase transition between the Kitaev spin liquid limit at $\phi/\pi = 0$ and the Γ_γ-only limit at $\phi/\pi = 0.5$. This result is clearly seen in the ground state energy and static structure factor (SSF) computed by exact diagonalization (ED) on a 24-site honeycomb cluster with $a = 0.1$. An independent calculation of the ground state energy and entanglement entropy on the infinite tree lattice with $a = 0.1$ by infinite time-evolution block decimation (iTEBD) shows no sign of a phase transition and supports the ED results.
2) An intervening magnetically ordered phase separates the spin liquid phase near the pure Γ_γ limit and the antiferromagnetic Kitaev spin liquid at $\phi/\pi = 1$.
3) The specific heat $C(T)$ and entropy $S(T)$ at finite temperatures computed by the method of thermal pure quantum states[31–35] (see Supplementary Materials) suggest a smooth crossover from the ferromagnetic Kitaev limit to the pure Γ_γ limit.
4) Zig-zag spin correlations become dominant upon perturbing the quantum spin liquid phase in $0 < \phi < \pi/2$ by J_3, suggesting significant enhancement of the zig-zag order for large J_3.

Extended spin liquid state in global phase diagram — The ground state energy per site E_0/N of Eq. (1) was computed for $\phi/\pi \in [0, 1]$, and for anisotropy parameters $a = 0$ and 0.1 by ED on a 24-site cluster using periodic boundary conditions (see Supplementary Materials). Divergences in $-\frac{1}{N}\frac{\partial^2 E_0}{\partial\phi^2}$ were used to identify possible phase transitions.

Sharp peaks of varying intensity can be identified in $-\frac{1}{N}\frac{\partial^2 E_0}{\partial\phi^2}$ throughout the phase space as shown in Fig. 1a for $a = 0.1$ (solid purple). Remarkably, when $\phi/\pi \in [0, 0.5]$ with slight anisotropy, the second derivative of the energy presents no sharp features suggesting that *the ground state of the Γ-limit* ($\phi/\pi = 0.5$) *is smoothly connected to the ferromagnetic Kitaev spin liquid* ($\phi/\pi = 0$). In the antiferromagnetic region of phase space, there are two large peaks in $-\frac{1}{N}\frac{\partial^2 E_0}{\partial\phi^2}$ encompassing a large region of phase space separating the Γ-limit and the exactly solvable antiferromagnetic Kitaev limit at $\phi/\pi = 1$. These peaks coincide with kinks in E_0/N (solid yellow) shown in Fig. 1a. Two smaller peaks can also be seen near $\phi/\pi = 0.75$, however these are not present in the $a = 0$ limit, while the larger peaks near $\phi/\pi = 0.5$ and 1 appear consistently for different a. The small peaks can thus be considered spurious and a consequence of the finite cluster size, with only one phase separating the Γ and antiferromagnetic Kitaev limits. Similar finite size effects were also found for $\phi/\pi \in [0, 0.5]$ when $a = 0$, as discussed in the Supplementary Materials, which makes it difficult to draw a conclusion on the phase diagram for the isotropic model ($a = 0$).

Magnetic order and perturbations — The ground state wavefunction of Eq. (1) computed by ED is used to evaluate real-space spin-spin correlation functions $\langle \mathbf{S}_i \cdot \mathbf{S}_j \rangle$, where i and j are site indices on the honeycomb lattice. By Fourier transform, we obtain the SSF given by $S_\mathbf{q} = \frac{1}{N}\sum_{i,j} e^{i(\mathbf{r}_i - \mathbf{r}_j)\cdot\mathbf{q}} \langle \mathbf{S}_i \cdot \mathbf{S}_j \rangle$ where $\mathbf{q}$ is a vector in the reciprocal lattice. The SSF at various points in the Brillouin zone (BZ) is plotted over the phase space in the bottom panel of Fig. 1a.

The discontinuities in the SSF can be directly matched with the divergences in $-\frac{1}{N}\frac{\partial^2 E_0}{\partial\phi^2}$. Visualizations of the SSF over the BZ for representative ϕ in the phase diagram are presented in Fig. 1b. The SSF in Fig. 1b is obtained by computing the average of $\langle S_i \cdot S_j \rangle$ over all n.n. bonds, 2nd n.n., etc. and perfoming the resulting one-dimensional Fourier transform. This calculation reflects the presence of different domains in the crystal, in which either of x, y, z bond interactions can be stronger and thus, over the whole crystal, these domains result in an isotropic S_q despite the inherent bond anistropy in Eq. (1). The SSF varies smoothly when $a = 0.1$ for $\phi \in [0, \pi/2]$ and the spin correlations at the Γ- and M-points are comparable in intensity when $\Gamma \simeq K_\gamma$, leading to a "star"-shaped structure in the SSF as seen in Fig. 1b (e.g, $\phi/\pi = 0.2$). The extended phase separating $\phi/\pi = 0.5$ and 1 is characterized

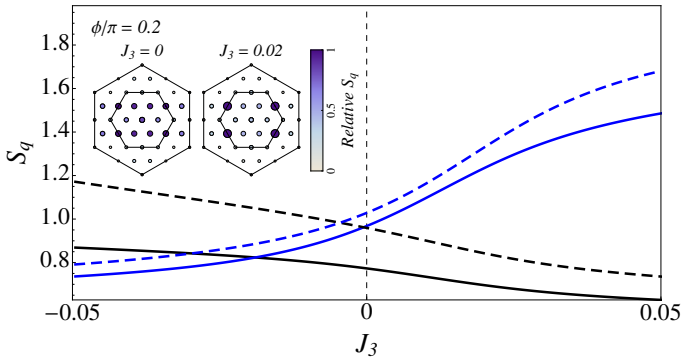

FIG. 2. (Color online) SSF at the Γ- (black) and M-points (blue) in the BZ for small J_3. Solid and dashed curves correspond to $\phi/\pi = 0.5$ and 0.2 respectively. The inset shows the dramatic change in the relative intensity at the Γ- and M-points for small $J_3 > 0$.

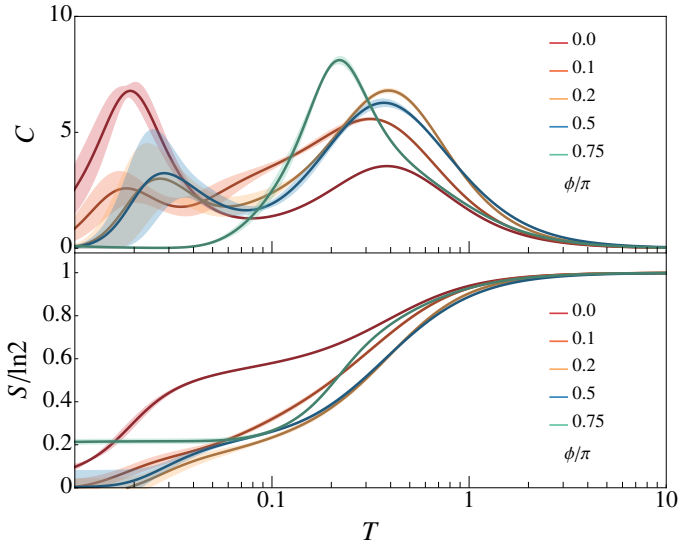

FIG. 3. (Color online) Results of the method of thermal pure quantum states on a 24-site cluster with anisotropy parameter $a = 0.1$. Plotted in solid curves are the temperature dependence of heat capacity $C(T)$ (top) and entropy $S(T)$ (bottom) for various ϕ in the phase diagram. The shaded regions represent the estimated errors on the results. The temperature T is expressed in units where $\sqrt{(K_z/(1+2a))^2 + \Gamma_z^2} = \sqrt{(K_{x,y}/(1-a))^2 + \Gamma_{x,y}^2} = 1$.

by dominating spin correlations at the K- and Γ′-points in the reciprocal lattice ($\phi/\pi = 0.75$ in Fig. 1b). Contained within this phase is the exactly solvable point with hidden $SU(2)$ symmetry at $\phi/\pi = 0.75$ which features K-point correlations[36] consistent with the results presented here. Furthermore, the energy spectrum (see Supplementary Materials) in this extended phase is qualitatively different from the rest of the phase space which, together with the peaks in $-\frac{1}{N}\frac{\partial^2 E_0}{\partial \phi^2}$ and changes in S_q, indicates that a real transition into this magnetically ordered state has occured. Thus the extended spin liquid phase for ferromagnetic K is separated from the antiferromagnetic Kitaev spin liquid at $\phi/\pi = 1$ by a magnetically ordered phase.

These results can be connected to real materials, particularly $RuCl_3$ in which a zig-zag magnetic ordering has been observed[37–39]. Previous studies have shown that in addition to the n.n. ferromagnetic Kitaev and antiferromagnetic Γ interactions, a 3rd n.n. antiferromagnetic Heisenberg interaction J_3 is non-vanishing and plays a role in determining the magnetic ordering in $RuCl_3$[26,27]. Fig. 2 shows that the effect of perturbing Eq. (1) by J_3 is to enhance (suppress) the M-point (Γ-point) spin correlations, consistent with a zig-zag magnetically ordered state observed in experiments. This result indicates that by tuning J_3 in the real material, an *alternate path to achieve a spin liquid phase may be realized.*

Specific heat and thermal entropy — Previous study on the finite temperature properties of the Kitaev model has shown that Kitaev spin liquids feature two peaks in the heat capacity $C(T)$ and a $\frac{1}{2}$-plateau in the entropy $S(T)$, which is attributed to the thermal fractionalization of spin degrees of freedom[40]. Here we go beyond the Kitaev limit and investigate the heat capacity and entropy at finite temperature in the presence of Γ, which is expected to compete with K_γ in $RuCl_3$, using the method of thermal pure quantum states (see Supplementary Materials).

The dependence of $C(T)$ on ϕ when $a = 0.1$ is plotted in the top panel of Fig. 3. The expected two peak structure in $C(T)$ is observed when $\phi/\pi = 0$, and is seen to be maintained continuously as ϕ/π approaches 0.5 so that the Γ-limit shows a qualitatively similar behaviour in $C(T)$ to the Kitaev spin liquid. Evidence for a phase transition can be seen when $\phi \gtrsim 0.7$ on account of the abrupt change in $C(T)$, resembling that of the heat capacity in trivially ordered phases[41]. This finding is consistent with our ED results and the 120-order at $\phi/\pi = 0.75$ seen in Refs. 14 and 36. The dependence of $S(T)$ on ϕ is plotted in the bottom panel of Fig. 3 with a clear $\frac{1}{2}$-plateau observed when $\phi/\pi = 0$, consistent with the expected Kitaev spin liquid behaviour. In addition, a plateau of about 1/5 the total entropy is observed when $\phi/\pi = 0.5$. Another plateau is observed in the magnetically ordered phase around $\phi/\pi = 0.75$; however, this feature can be attributed to finite-size effects as follows. The $(N+1)$-fold ground state degeneracy at $\phi/\pi = 0.75$ due to the hidden $SU(2)$ symmetry[36] is only slightly broken away from this point, inducing a plateau in $S(T)$ with height given by $\ln(N+1)/N\ln 2 \simeq 0.1935 \sim 1/5$ when $N = 24$. By contrast, the height of the plateau around $\phi/\pi = 0.5$ is independent of N[42].

The physical origin of the two peak structure in $C(T)$ and the plateau in $S(T)$ can be traced to the energy scales of the thermal fluctuations of the underlying quasiparticles in the spin liquid[40]. In the Kitaev spin liquid at zero temperature, the low-lying quasiparticle excitations are characterized by itinerant Majorana fermions which disperse in a background of zero flux[19,43]. It has been shown that as temperature increases, the flux degrees of freedom begin to fluctuate and lead to the low temperature peak seen in $C(T)$. These fluctuating fluxes utlimately increase the entropy of the system, resulting in the plateau seen in $S(T)$. Furthermore, the high temperature peak in $C(T)$ is attributed to the development of short range spin correlations and above this temperature scale, the system enters a classical paramagnetic state[40]. Our results show that the two-peak structure in $C(T)$, and corresponding entropy

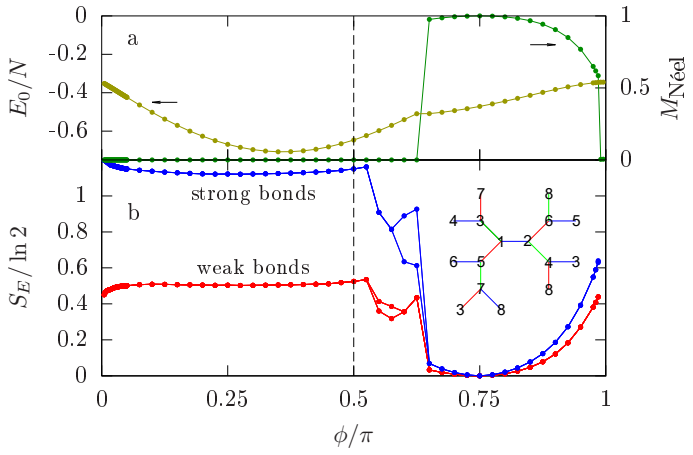

FIG. 4. (Color online) iTEBD results for small anisotropy $a = 0.1$, and bond dimension $\chi = 10$. (a) Néel order parameter, $M_{\text{Néel}}$ and ground state energy per site, E_0/N. In the ordered region, the moments align along the [111] direction. (b) Entanglement entropy S_E associated with splitting the system along the different bonds in the eight-site unit cell. In most of the phase diagram all the strong z bonds are identical, and so are all the weak, x and y bonds. In the transition region near $\phi = 0.6\pi$, the symmetry between like bonds is broken, perhaps indicating a first order transition. At $\phi/\pi = 0.75$, the entanglement entropy vanishes since the system is in a product state. Inset: schematic of Cayley tree with $z = 3$ connectivity.

plateau, is qualitatively maintained when interpolating between the Kitaev spin liquid phase and the Γ-limit, further suggesting that no phase transition has taken place.

Similarities on the infinite tree — We further studied Eq. (1) on an infinite Cayley tree with $z = 3$ connectivity, using the infinite time-evolving block decimation algorithm[44] (iTEBD; see Supplementary Materials). Classically, the ground state in the Γ-limit on the infinite tree is macroscopically degenerate because a different state with the same energy can be constructed by flipping the sign of one spin component on an infinite string of neighboring spins. For example, in the inset of Fig. 4, we can flip the signs of $\{\dots S_7^y, S_3^x, S_1^z, S_2^y, S_6^x, S_8^z \dots\}$, and obtain a new state with the same energy. For a finite tree, the number of paths one can construct scales with the size of the boundary, which is extensive. The Γ-limit on the two-dimensional (2D) honeycomb and three-dimensional (3D) hyper-honeycomb[25] lattices also feature similar classical degeneracy. The similarity at the classical level of the Γ-limit on the infinite tree to the 2D and 3D lattices prompts us to study the quantum model on the infinite tree for further insight. Figure 4 shows results of the eight-site iTEBD calculation with bond dimension $\chi = 10$, and anisotropy $a = 0.1$. In this calculation, we have also introduced an anisotropy to Γ_γ such that $\Gamma_x = \Gamma_y = (1-a)\sin\phi$ and $\Gamma_z = (1+2a)\sin\phi$ in order to apply the iTEBD method (see Supplementary Materials). No transition is found when $\phi/\pi \in [0, 0.5]$ and the obtained state is a highly entangled paramagnet, with $S_E \sim 0.8$ for strong (z) bonds, while for weak (x, y) bonds, $S_E \sim 0.4$. Deep in the gapped phase of the Kitaev model, with large anisotropy a, one finds $S_E \sim \log 2 \sim 0.693$ for the strong bonds and much smaller values of S_E for the weak bonds. Both, however, increase as the anisotropy is reduced - perhaps due to a finite contributions from the Majorana fermions[45]. An increase is expected in the entanglement entropy as one approaches a phase transition, usually related to the closing of an excitation gap, however no such peaks are seen for $0 < \phi < \pi/2$. Similarly, there are no sharp features in the ground state energy E_0 as a function of ϕ, which indicates that this phase is smoothly connected to the Kitaev spin liquid at $\phi = 0$.

There is an apparent first order transition around $\phi = 0.6\pi$ into a Néel state with spins ordered in the [111] direction, accompanied by a dramatic lowering of S_E on both strong and weak bonds into this region. This Néel state becomes a simple product state when $\phi/\pi = 0.75$, as seen by the vanishing of S_E. Due to a hidden $SU(2)$ symmetry, a 120 order state[14,36] is expected on the isotropic honeycomb lattice at this point; however, this state is not compatible with the eight site unit cell tree lattice, and a Néel product stateis selected instead. A final transition into a paramagnetic state is seen before the antiferromagnetic Kitaev limit, so that there are *three phases* observed on the infinite tree, in direct similarity to the ED results on the honeycomb lattice above.

Discussion – The highlight of our numerical results is that there exists an extended family of spin liquid phases, which may be smoothly connected to the ferrmagnetic Kitaev spin liquid and the introduction of J_3 would greatly favor a transition from such a quantum spin liquid phase into the zig-zag ordered phase. As briefly mentioned earlier, this is precisely the regime where our model is relevant to physics of $RuCl_3$. In a recent inelastic neutron scattering experiment on $RuCl_3$, it is found that the continuum of finite energy excitations exists both below and above the magnetic transition temperature despite that the low temperature ground state is the zig-zag long-range ordered state[30]. The inelastic neutron scattering data for the continuum show the star-shape intensity that extends from the zone center towards the M points of the Brillouin zone. This would represent the remnant short-range spin correlations which exist both below and above the transition temperature.

Recall that the static structure factor in our ED study shows enhanced (decreased) short-range spin correlations at the M point (zone center) of the Brillouin zone as one moves from the ferromagnetic Kitaev limit to the pure Γ_γ limit. When the strength of the ferromagnetic Kitaev interaction and the Γ_γ interaction become comparable, both of the short-range spin correlations at the M and the zone center would show significant intensity, which leads to the star-shape structure in momentum space. This behavior may be favorably compared to the finite-energy short-range spin correlations seen in $RuCl_3$. Given that the *ab initio* computations suggest comparable magnitudes of the ferromagnetic Kitaev and Γ_γ interactions in $RuCl_3$[26], it is conceivable that $RuCl_3$ may be very close to the quantum spin liquid phase found in our model. As shown in our work, the introduction of small J_3 would greatly favor the zig-zag magnetically ordered phase as observed in $RuCl_3$.

Another implication of our work may be found in a recent high pressure experiment on β-Li_2IrO_3, where the Ir^{4+} ions carrying the pseudospin-1/2 sit on the three-dimensional hyperhoneycomb lattice[13]. The local connectivity of this

lattice is the same as the honeycomb lattice while the smallest loop here is a ten-sided loop. The spin interactions in this system is also described by the Kitaev, Γ_γ, and antiferromagnetic Heisenberg interactions. At ambient pressure, the material is in a complex spiral magnetically ordered phase. Upon applying the hydrostatic pressure, the magnetic order disappears at 2.5GPa[13] and the NMR experiment suggests that the system may be in a quantum spin liquid phase[46]. On the other hand, a recent *ab initio* computation shows that the spin interactions under high pressure favors the Γ_γ interaction and the antiferromagnetic interaction becomes negligibly small[47]. Hence again the Kitaev-Γ model becomes relevant in β-Li_2IrO_3 under high pressure. While our ED study is done on the two-dimensional honeycomb lattice, the iTEBD result on the infinite tree lattice would strongly suggest that the spin liquid phenomenology found in the honeycomb lattice may also be applicable to the hyper-honeycomb system. That is, the quantum spin liquid obtained by applying high pressure may be smoothly connected to the Kitaev spin liquid phase.

Finally, more analytical understanding of the connection between the pure Kitaev limit and the quantum spin liquid phases identified in our numerical work would be extremely valuable for future applications on real materials. This would be an excellent topic for future study.

Acknowledgements

This work was supported by the NSERC of Canada and the Center for Quantum Materials at the University of Toronto. Y. Y. was supported by JSPS KAKENHI (Grant Nos. 15K17702 and 16H06345) and was supported by PRESTO, JST. Y. Y. was also supported in part by MEXT as a social and scientific priority issue (Creation of new functional devices and high-performance materials to support next-generation industries) to be tackled by using post-K computer. Computations were mainly performed on the GPC supercomputer at the SciNet HPC Consortium. SciNet is funded by: the Canada Foundation for Innovation under the auspices of Compute Canada; the Government of Ontario; Ontario Research Fund - Research Excellence; and the University of Toronto. We thank helpful discussions with Frank Pollmann, Matthias Gohlke, Shunsuke Furukawa, and Subhro Bhattacharjee. We particularly thank Natalia Perkins and Ioannis Rousochatzakis for informing us of their unpublished ED results on related models.

[1] L. Balents, Nature **464**, 199 (2010).
[2] Y. Shimizu, K. Miyagawa, K. Kanoda, M. Maesato, and G. Saito, Phys. Rev. Lett. **91**, 107001 (2003).
[3] J. S. Helton, K. Matan, M. P. Shores, E. A. Nytko, B. M. Bartlett, Y. Yoshida, Y. Takano, A. Suslov, Y. Qiu, J.-H. Chung, D. G. Nocera, and Y. S. Lee, Phys. Rev. Lett. **98**, 107204 (2007).
[4] Y. Okamoto, M. Nohara, H. Aruga-Katori, and H. Takagi, Phys. Rev. Lett. **99**, 137207 (2007).
[5] M. Yamashita, N. Nakata, Y. Senshu, M. Nagata, H. M. Yamamoto, R. Kato, T. Shibauchi, and Y. Matsuda, Science **328**, 1246 (2010).
[6] T.-H. Han, J. S. Helton, S. Chu, D. G. Nocera, J. A. Rodriguez-Rivera, C. Broholm, and Y. S. Lee, Nature **492**, 406 (2012).
[7] G. Jackeli and G. Khaliullin, Phys. Rev. Lett. **102**, 017205 (2009).
[8] W. Witczak-Krempa, G. Chen, Y. B. Kim, and L. Balents, Annual Review of Condensed Matter Physics **5**, 57 (2013).
[9] J. G. Rau, E. K.-H. Lee, and H.-Y. Kee, Annual Review of Condensed Matter Physics **7**, 195 (2016).
[10] Y. Singh, S. Manni, J. Reuther, T. Berlijn, R. Thomale, W. Ku, S. Trebst, and P. Gegenwart, Phys. Rev. Lett. **108**, 127203 (2012).
[11] K. Plumb, J. Clancy, L. Sandilands, V. Vijay Shankar, Y. Hu, K. Burch, H.-Y. Kee, and Y.-J. Kim, Phys. Rev. B **90**, 041112 (2014).
[12] K. A. Modic, T. E. Smidt, I. Kimchi, N. P. Breznay, A. Biffin, S. Choi, R. D. Johnson, R. Coldea, P. Watkins-Curry, G. T. McCandless, J. Y. Chan, F. Gandara, Z. Islam, A. Vishwanath, A. Shekhter, R. D. McDonald, and J. G. Analytis, Nature Communications **5**, 4203 (2014).
[13] T. Takayama, A. Kato, R. Dinnebier, J. Nuss, H. Kono, L. Veiga, G. Fabbris, D. Haskel, and H. Takagi, Phys. Rev. Lett. **114**, 077202 (2015).
[14] J. G. Rau, E. K.-H. Lee, and H.-Y. Kee, Phys. Rev. Lett. **112**, 077204 (2014).
[15] S. H. Chun, J.-W. Kim, J. Kim, H. Zheng, C. Stoumpos, C. Malliakas, J. Mitchell, K. Mehlawat, Y. Singh, Y. Choi, T. Gog, A. Al-Zein, M. Sala, M. Krisch, J. Chaloupka, G. Jackeli, G. Khaliullin, and B. J. Kim, Nat. Phys. **11**, 462 (2015).
[16] H.-S. Kim, V. V. Shankar, A. Catuneanu, and H.-Y. Kee, Phys. Rev. B **91**, 241110(R) (2015).
[17] E. K.-H. Lee and Y. B. Kim, Phys. Rev. B **91**, 064407 (2015).
[18] E. K.-H. Lee, J. G. Rau, and Y. B. Kim, Phys. Rev. B **93**, 184420 (2016).
[19] A. Kitaev, Ann. Phys. **321**, 2 (2006).
[20] J. Chaloupka, G. Jackeli, and G. Khaliullin, Phys. Rev. Lett. **105**, 027204 (2010).
[21] H.-C. Jiang, Z.-C. Gu, X.-L. Qi, and S. Trebst, Phys. Rev. B **83**, 245104 (2011).
[22] R. Schaffer, S. Bhattacharjee, and Y. B. Kim, Phys. Rev. B **86**, 224417 (2012).
[23] C. Price and N. B. Perkins, Phys. Rev. B **88**, 024410 (2013).
[24] M. Gohlke, R. Verresen, R. Moessner, and F. Pollmann, arXiv:1701.04678 [cond-mat] (2017), arXiv: 1701.04678.
[25] I. Rousochatzakis and N. B. Perkins, arXiv:1610.08463 [cond-mat] (2016), arXiv: 1610.08463.
[26] H.-S. Kim and H.-Y. Kee, Phys. Rev. B **93**, 155143 (2016).
[27] S. M. Winter, Y. Li, H. O. Jeschke, and R. Valenti, Phys. Rev. B **93**, 214431 (2016).
[28] R. Yadav, N. A. Bogdanov, V. M. Katukuri, S. Nishimoto, J. van den Brink, and L. Hozoic, Scientific Reports **6**, 37925 (2016).
[29] A. Catuneanu, H.-S. Kim, O. Can, and H.-Y. Kee, Phys. Rev. B **94**, 121118(R) (2016).
[30] A. Banerjee, J. Yan, J. Knolle, C. A. Bridges, M. B. Stone, M. D. Lumsden, D. G. Mandrus, D. A. Tennant, R. Moessner, and S. E. Nagler, arXiv preprint arXiv:1609.00103 (2016).
[31] M. Imada and M. Takahashi, J. Phys. Soc. Jpn. **55**, 3354 (1986).
[32] J. Jaklic and P. Prelovsek, Phys. Rev. B **49**, 5065 (1994).
[33] A. Hams and H. De Raedt, Phys. Rev. E **62**, 4365 (2000).
[34] S. Sugiura and A. Shimizu, Phys. Rev. Lett. **108**, 240401

(2012).
[35] S. Sugiura and A. Shimizu, Phys. Rev. Lett. **111**, 010401 (2013).
[36] J. Chaloupka and G. Khaliullin, Phys. Rev. B **92**, 024413 (2015).
[37] J. A. Sears, M. Songvilay, K. W. Plumb, J. P. Clancy, Y. Qiu, Y. Zhao, D. Parshall, and Y.-J. Kim, Phys. Rev. B **91**, 144420 (2015).
[38] R. D. Johnson, S. C. Williams, A. A. Haghighirad, J. Singleton, V. Zapf, P. Manuel, I. I. Mazin, Y. Li, H. O. Jeschke, R. Valentí, and R. Coldea, Phys. Rev. B **92**, 235119 (2015).
[39] H. Cao, A. Banerjee, J.-Q. Yan, C. Bridges, M. Lumsden, D. Mandrus, D. Tennant, B. Chakoumakos, and S. Nagler, Phys. Rev. B **93**, 134423 (2016).
[40] J. Nasu, M. Udagama, and Y. Motome, Phys. Rev. B **92**, 115122 (2015).
[41] Y. Yamaji, T. Suzuki, T. Yamada, S.-i. Suga, N. Kawashima, and M. Imada, Phys. Rev. B **93**, 174425 (2016).
[42] The height of the plateau in the temperature dependence of entropy is also examined by using a 32 site cluster.
[43] J. Knolle, D. Kovrizhin, J. Chalker, and R. Moessner, Phys. Rev. Lett. **112**, 207203 (2014).
[44] G. Vidal, Phys. Rev. Lett. **98**, 070201 (2007).
[45] I. Kimchi, J. G. Analytis, and A. Vishwanath, Phys. Rev. B **90**, 205126 (2014).
[46] H. Takagi, a talk given at the workshop Novel States in Spin-Orbit Coupled Quantum Matter: from Models to Materials, held in Kavli Institute for Theoretical Physics, University of California at Santa Barbara, July 27-31, 2015.
[47] H.-S. Kim, Y. B. Kim, and H.-Y. Kee, Phys. Rev. B **94**, 245127 (2016).